European Journal of Medicinal Chemistry 70 (2013) 623–630

Contents lists available at ScienceDirect

European Journal of Medicinal Chemistry

journal homepage: http://www.elsevier.com/locate/ejmech

Original article

Novel coumarin-3-carboxamides bearing *N*-benzylpiperidine moiety as potent acetylcholinesterase inhibitors

Ali Asadipour [a], Masoumeh Alipour [b], Mona Jafari [b], Mehdi Khoobi [b], Saeed Emami [c], Hamid Nadri [d,e], Amirhossein Sakhteman [d,e], Alireza Moradi [d,e], Vahid Sheibani [a], Farshad Homayouni Moghadam [e], Abbas Shafiee [b], Alireza Foroumadi [a,b,*]

[a] *Neuroscience Research Center, Kerman University of Medical Sciences, Kerman, Iran*
[b] *Department of Medicinal Chemistry, Faculty of Pharmacy and Pharmaceutical Sciences Research Center, Tehran University of Medical Sciences, Tehran, Iran*
[c] *Department of Medicinal Chemistry and Pharmaceutical Sciences Research Center, Faculty of Pharmacy, Mazandaran University of Medical Sciences, Sari, Iran*
[d] *Department of Medicinal Chemistry, Faculty of Pharmacy, Shahid Sadoughi University of Medical Sciences, Yazd, Iran*
[e] *Neurobiomedical Research Center, School of Medicine, Shahid Sadoughi University of Medical Sciences, Yazd, Iran*

ARTICLE INFO

Article history:
Received 18 May 2013
Received in revised form
7 October 2013
Accepted 10 October 2013
Available online 23 October 2013

Keywords:
Acetylcholinesterase
Butyrylcholinesterase
Coumarin
N-Benzylpiperidine
Alzheimer's disease
Docking
Kinetic study

ABSTRACT

Some novel coumarin-3-carboxamide derivatives linked to *N*-benzylpiperidine scaffold were synthesized and evaluated as acetylcholinesterase (AChE) and butyrylcholinesterase (BuChE) inhibitors. The screening results showed that most of compounds exhibited potent anti-AChE activity in the range of nM concentrations. Among them, compound **10c** bearing an *N*-ethylcarboxamide linker and a 6-nitro substituent showed the most potent activity (IC_{50} = 0.3 nM) and the highest selectivity (SI = 26,300). Compound **10c** was 46-fold more potent than standard drug donepezil against AChE. The kinetic study revealed that compound **10c** exhibited mixed-type inhibition against AChE. Protein-ligand docking study demonstrated that the target compounds have dual binding site interaction mode and these results are in agreement with kinetic study.

1. Introduction

Alzheimer's disease (AD) is a neurodegenerative disease with symptoms of memory loss, cognition defect and behavioral impairment [1]. AD is mainly characterized by the pre-synaptic decrease of acetylcholine (ACh) due to damage of cholinergic neurons in some especial parts of the brain such as hippocampus and cortex (cholinergic hypothesis) [2,3]. Concerning the cholinergic hypothesis one of the rational and effective approaches to treat the AD's symptoms, is raising the ACh through inhibition of acetylcholinesterase (AChE) that is responsible for hydrolysis of ACh in pre-synaptic areas [4]. Moreover, it has been recently reported that dual inhibition of AChE and butyrylcholinesterase (BuChE) might improve the signs of AD and symptoms owing to the key role of BuChE in hydrolysis of ACh. Indeed in damaged brain, preserving the AChE/BuChE activity ratios is essential for successful treatment of AD [5,6]. Based on these findings, several AChE inhibitors comprising different chemical scaffolds such as donepezil [7], galantamine [8] and ensaculin [9] were synthesized and used clinically to prevent progression of AD in early stages (Fig. 1).

Previously, due to the straightforward functionalization of coumarin ring, several coumarin derivatives have been prepared and evaluated as AChE inhibitors [10]. It has been observed that coumarins such as AP2238 (Fig. 1) encompassing substitution at position 3 or 4 have shown increased activity against AChE rather than 6 or 7 substituted coumarins [10].

Regarding the X-ray crystallographic structure of AChE (PDB ID: 1EVE), three main binding sites are determined: the catalytic triad at the bottom of active site including Ser200, His440, and Glu327, the catalytic anionic site (CAS) at the vicinity of the catalytic triad

* Corresponding author. Department of Medicinal Chemistry, Faculty of Pharmacy and Pharmaceutical Sciences Research Center, Tehran University of Medical Sciences, Tehran, Iran. Tel.: +98 21 66954708; fax: +98 21 66461178.
E-mail addresses: aforoumadi@yahoo.com, aforoumadi@tums.ac.ir (A. Foroumadi).

0223-5234/$ – see front matter © 2013 Elsevier Masson SAS. All rights reserved.
http://dx.doi.org/10.1016/j.ejmech.2013.10.024

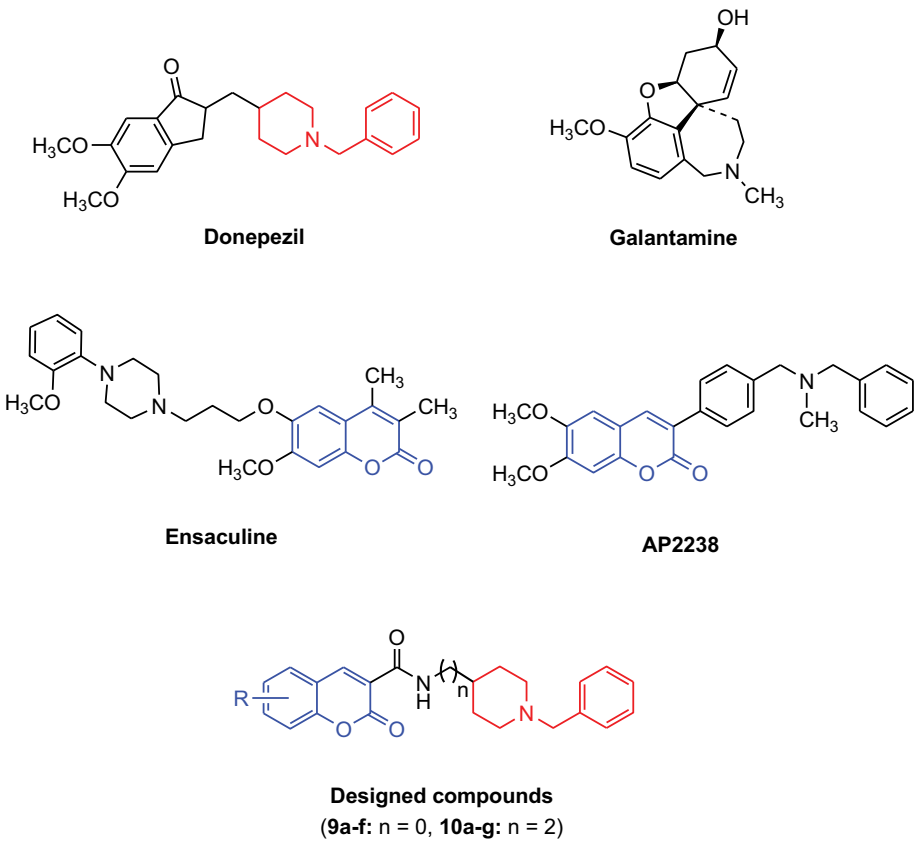

Fig. 1. Structures of well-known cholinesterase inhibitors and designed compounds.

consisting of Trp84, Tyr130, Gly199, His441, His444 and peripheral anionic site (PAS) at the gorge rim comprising Tyr70, Asp72, Tyr121, Trp279 and Tyr334. Furthermore, the key residue Phe330 in the midgorge is also involved in the recognition of ligands [11,12]. It was proved that dual binding site (DBS) AChE inhibitors were more potent inhibitors compared to the compounds that interact with only one site of the enzyme [13]. Several studies have shown that coumarin moiety can bind primarily to PAS of AChE [10]. Accordingly, different groups such as benzylamino, phenylpiperazine, and aniline, which interact with the catalytic site, have been successfully connected to the coumarin scaffold using different spacers to obtain dual binding site inhibitors [14]. In continuation of our previous work on coumarin AChE inhibitors [15], a novel series of coumarins have been designed through hybridization approach in which *N*-benzylpiperidine moiety of donepezil as a CAS binder and the coumarin scaffold as PAS binding core were connected together with amide linker (Fig. 1). Herein, the synthesis, biological evaluation and *in silico* studies of some substituted coumarins **9a**–**f** and **10a**–**g** as novel dual binding site inhibitors of AChE are reported.

2. Results and discussion

2.1. Chemistry

The synthetic routes from key intermediates **3a**–**g** and **8a**,**b** to target compounds **9a**–**f** and **10a**–**g** have been shown in Scheme 1. Initially, several ethyl coumarin-3-carboxylate derivatives **2a**–**g** were synthesized using commercial 2-hydroxybenzaldehydes **1a**–**g** and diethylmalonate in the presence of catalytic amount of piperidine which was then hydrolyzed with aqueous solution of sodium hydroxide to furnish the corresponding coumarin-3-carboxylic acid **3a**–**g** (Supplementary material) [16]. The amine intermediate 2-(1-benzylpiperidin-4-yl)ethanamine (**8b**) was prepared from commercially available 1-benzyl-4-piperidone (**4**) and malonitrile in 60% yield over four steps [17]. Thus, simple condensation of malonitrile with compound **4** provided 2-(1-benzylpiperidin-4-ylidene)malononitrile (**5**). The latter compound was then converted to ethyl cyanoacetate **6** through reduction and simultaneous formation of esteric bond. Then, compound **8b** can be prepared from hydrolysis and decarboxylation of compound **6** followed by reduction with $LiAlH_4$ (Supplementary material).

Finally, coumarin-3-carboxylic acids **3a**–**g**, were chlorinated using thionyl chloride to give the appropriate coumarin-3-carbonyl chloride and then coupled with 1-benzylpiperidin-4-amine **8a** or 2-(1-benzylpiperidin-4-yl)ethanamine **8b** to yield corresponding amides **9** or **10** in moderate yields, respectively (Scheme 1). Activation of the

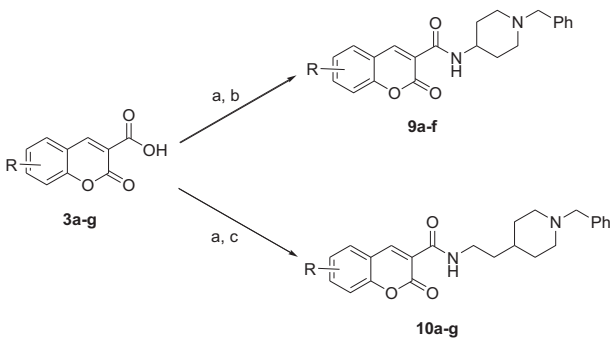

Scheme 1. Synthesis of target compounds **9** and **10**. Reagents and conditions: (a) thionyl chloride, reflux; (b) 1-benzylpiperidin-4-amine (**8a**), K_2CO_3, toluene, reflux; (c) 2-(1-benzylpiperidin-4-yl) ethanamine (**8b**), K_2CO_3, toluene, reflux.

carboxylic groups of coumarin-3-carboxylic acids **3a**–**g** were screened by various reagents like *N*-(3-dimethylaminopropyl)-*N*′-ethylcarbodiimide hydrochloride (EDC), carbonyldiimidazole (CDI) and dicyclohexylcarbodiimide (DCC) in various solvents, but the best result was obtained by using thionyl chloride.

Structural elucidations of all compounds were done using ^{1}H NMR and IR spectroscopy and elemental analysis for H, C and N.

2.2. Pharmacology

2.2.1. Inhibitory activity against AChE and BuChE

The inhibitory activity of the target compounds against AChE and BuChE is displayed in Table 1. Based on the IC_{50} values for AChE, all compounds with the exception of **9a** and **9f** exhibited potent activity in the range of sub-micromolar concentrations (0.3–633 nM). However, compound **9a** and **9f** with IC_{50} values of 1.2–1.7 μM had remarkable anti-AChE activity.

The designed compounds are composed of two fragments; a CAS binding motif (*N*-benzylpiperidine) and a PAS binding motif (coumarin) which are joined either via a carboxamide (compounds **9a**–**f**) or *N*-ethylcarboxamide (compounds **10a**–**g**) linkers. It was observed that all compounds with *N*-ethylcarboxamide linker are more active than their counterparts with carboxamide linker. The most active derivative in this series was compound **10c** bearing a nitro group at position 6 of the coumarin ring (IC_{50} = 0.3 nM).

The IC_{50} values of substituted coumarins against AChE were significantly less than those of corresponding unsubstituted coumarins **9a** and **10a**. These data revealed that the bromo, nitro, and methoxy substituents increase the anti-AChE activity. Exceptionally, introduction of hydroxyl group on the 6- or 7-position of coumarin ring diminishes the inhibitory activity against AChE. The comparison of the IC_{50} values of 7-methoxy analogs **9d** and **10e** with those of 7-hydroxy counterparts **9f** and **10f** demonstrated that *O*-methylation of 7-hydroxycoumarins improved the activity. The 8-methoxycoumarin derivative **10g** with IC_{50} of 2 nM was more active than its 7-methoxy isomer **10e** (IC_{50} = 5 nM). In contrast, in the *N*-(1-benzylpiperidin-4-yl)-carboxamide series, the AChE inhibitory activity of 7-methoxy analog **9d** was superior to 8-methoxy isomer **9e**.

The IC_{50} values of *N*-(1-benzylpiperidin-4-yl)-carboxamide series (compounds **9a**–**f**) against BuChE were ≥20 μM. Among the *N*-ethylcarboxamide series (compounds **10a**–**g**), compounds **10a**, **10b** and **10e** showed high inhibitory activity against BuChE with IC_{50} values ≤420 nM. The 7-methoxycoumarin **10e** was the most active compound against BuChE (IC_{50} = 357 nM). Interestingly, the comparison of anti-cholinesterase activities of 7- and 8-methoxy isomers **10e** and **10g** revealed that the position of methoxy group had high impact on BuChE/AChE selectivity (71 versus 9000).

It is worthwhile to note that the highest selectivity index was attributed to the most active compound against AChE, **10c** with 6-nitro substituent (SI = 26,300). Compound **10c** was 46-fold more potent than standard drug donepezil against AChE. Besides 6-nitro-compound **10c**, 6-bromo-, 7-methoxy-, and 8-methoxy-derivatives (compounds **10b**, **10e** and **10g**, respectively) in the *N*-ethyl-carboxamide series exhibited superior anti-AChE activity respect to donepezil.

However, it has been recently reported that dual inhibition of AChE/BuChE might improve the signs of AD [5,6]. Among the synthesized compounds, compound **10a** was shown to be dual cholinesterase inhibitor with more favorable balancing between AChE/BuChE inhibitions compared to the standard drug donepezil. In this point of view, compound **10a** prototype could be considered as promising lead for future studies.

2.2.2. Protection against H_2O_2-induced cell death in PC12 neurons

The neuroprotective activity of the selected compounds (**10b**, **10c** and **10e**) against oxidative stress-induced cell death in differentiated PC12 cells was evaluated. Thus, differentiated PC12 cells were pretreated with different concentrations (1, 10 and 100 μM) of the compounds and quercetine as reference compound for 3 h, before treatment with H_2O_2 (250 μM). H_2O_2 was added to the medium for induction of apoptosis and occurrence of apoptosis was established after staining with DAPI, and cell viability was measured after 24 h by using the MTT (3-(4,5-dimethylthiazol-2-yl)-2,5-diphenyltetrazolium bromide) assay. It should be mentioned that the selected compounds did not show any toxicity at concentrations of 1–100 μM. Therefore, neuroprotective activity of the compounds were evaluated within the range of 1–100 μM. Based on the results (Fig. 2), H_2O_2 significantly reduced the cell viability to 47% compared with control, whereas pretreatment with the compounds significantly protected neurons against cell death in all used concentrations (*P* value <0.05).

2.3. Docking studies

Docking studies were performed in order to obtain more insight into the binding mode of the compounds and also elucidate the influence of structural modifications on the inhibitory activities of the compounds against AChE. Several Ligand-bounded crystallographic structures of AChE are available. For the docking procedure, the pdb structure of 1EVE was taken from the Brookhaven protein database (http://www.rcsb.org) as a complex bound with inhibitor donepezil. To confirm the validity of the used docking protocol, the crystal structure of donepezil was re-docked on the target enzyme and the RMSD value (0.75 Å) showed the predictive ability of the used method.

Subsequently, the two most active compounds of each category (**9b**, **10c**) were subjected to Autodock vina 1.1.1 using the optimized parameters. As shown in Fig. 3, the orientation of both compounds in the active site was much similar to that of donepezil.

Since the piperidine moiety of the ligands is protonated at physiologic pH (7.4), the ligands were recognized by the anionic

Table 1
The IC_{50} values of the target compounds **9a**–**f** and **10a**–**g** against AChE and BuChE.

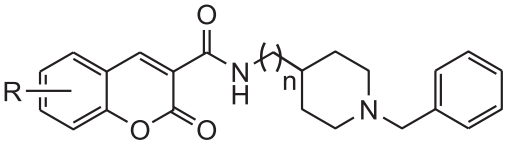

Compound	R	*n*	IC_{50}[a] (nM)		SI[d]
			AChE[b]	BuChE[c]	
9a	H	0	1200	17,000	14
9b	6-Br	0	30	42,000	1400
9c	6-NO_2	0	430	22,000	51
9d	7-OMe	0	183	27,000	147
9e	8-OMe	0	633	20,000	32
9f	7-OH	0	1700	55,000	32
10a	H	2	26	371	14
10b	6-Br	2	2	420	210
10c	6-NO_2	2	0.3	7900	26,300
10d	6-OH	2	70	15,610	222
10e	7-OMe	2	5	357	71
10f	7-OH	2	143	46,000	321
10g	8-OMe	2	2	18,000	9000
Donepezil			14	5380	384

[a] IC_{50} values are mean of the three independent experiments.
[b] AChE from *Electrophorus electricus*.
[c] BuChE from equine serum.
[d] SI = selectivity index (IC_{50} BuChE/IC_{50} AChE).

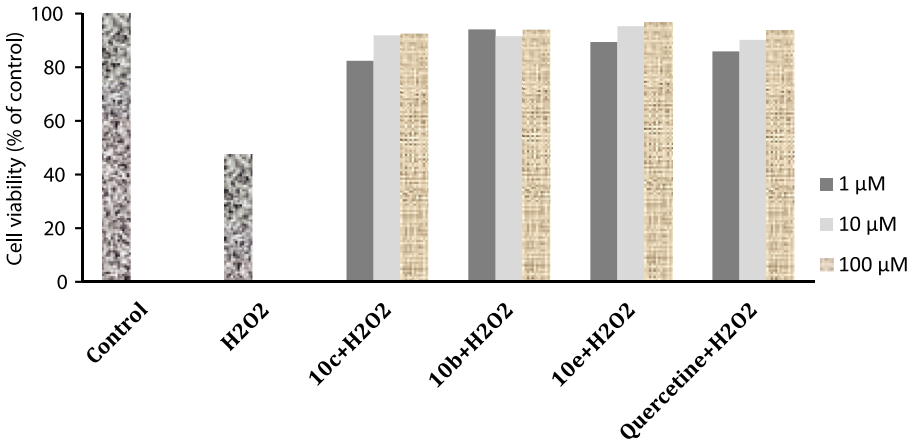

Fig. 2. Neuroprotective activity of compounds **10b**, **10c** and **10e** against H_2O_2-induced cell death in PC12 neurons. Differentiated PC12 cells were treated with different concentrations (1–100 μM) of the compound for 3 h. After 24 h, cell viability was determined by MTT assay in the presence H_2O_2. Quercetine was used as reference drug.

subsite of the enzyme. It was reported that, this feature of the molecules takes part in recognition and orientation of the ligands towards the active site [12]. Furthermore, it was observed that the benzyl moiety is oriented towards the CAS of the enzyme. It was therefore concluded that the compounds are anchored in the mid-gorge of the enzyme through *N*-benzylpiperidine fragment, while the coumarin parts of the molecules are accommodated in the gorge rim. A more detailed view for the interaction of the two compounds **9b** and **10c** is also displayed in Fig. 4. As presented, the phenyl ring of benzyl moiety in both compounds is in parallel disposition to Trp84 showing aromatic π–π interaction. Two other similar interactions including a π–cation between the quaternary nitrogen of piperidine ring with Phe330 and a π–π stacking of coumarin ring and Trp279 were also observed (Figs. 4 and 5). Compound **10c** displayed a hydrogen bond interaction between carbonyl group of coumarin moiety and the hydroxyl group of Tyr121. Consequently, the carbonyl part of amide group is oriented towards the hydrophilic pocket composed of Ser286, Phe290, and Arg289. These additional interactions were not observed in **9b**. It seems that the more flexibility of the *N*-ethylcarboxamide linker in **10c** led to its better interactions with the enzyme compared to **9b**. The higher potency of the compounds with *N*-ethylcarboxamide linker could be due to the more favorable interactions of compounds with the target enzyme.

2.4. Kinetic of the enzyme inhibition

The kinetic studies for the most active compound **10c**, were carried out at three fixed inhibitor concentrations (0.357 nM, 3.57 nM and 11.9 nM). In each case, the initial velocity measurements were achieved at different substrate (S), acetylthiocholine (ATCh) concentrations and the reciprocal of the initial velocity (1/v) was plotted against the reciprocal of [ATCh] [18]. The double-reciprocal (Lineweaver–Burk) plot showed a pattern of increasing slopes and increasing intercepts with higher inhibitor concentration (Fig. 6). This pattern indicates mixed-type of inhibition for **10c** resulting from a more enhanced inhibitor interaction with both the free enzyme and the acetylated enzyme.

3. Conclusion

A series of novel coumarin derivatives bearing *N*-benzylpiperidinyl moiety were synthesized and evaluated for AChE and BuChE inhibitory activity using a modified Ellman's method. The results showed that most of compounds exhibited potent anti-AChE activity. Among the synthesized derivatives, compound **10c** bearing an *N*-ethylcarboxamide linker and a 6-nitro substituent was the most active compound (IC_{50} = 0.3 nM) with high selectivity (SI = 26,300). Docking studies have also revealed that the higher flexibility of *N*-ethylcarboxamide linker in compound **10c** prototype might lead to the more facile accommodation of the compounds in the active site and dual binding site inhibition of the enzyme. Moreover, the neuroprotective activity of the target compounds against oxidative stress-induced cell death as an additional effect might be important for AD management.

4. Experimental

4.1. Chemistry

All commercially available starting materials and reagents were from Merck and were used without further purification. Coumarin-3-carboxylic acid derivatives **3a**–**g** were synthesized by using reported method [16]. Compound **8** was prepared from commercially available 1-benzyl-4-piperidone **4** and malonitrile according to the literature method [17]. Thin-layer chromatography was performed using silica gel 250 micron, F254 plates. Melting points were measured on a Kofler hot stage apparatus and are uncorrected. The IR spectra were recorded using Nicolet FT-IR Magna 550 spectrograph (KBr disks). ^{1}H NMR spectra were recorded on an NMR instrument Bruker 400 or 500 MHz. The chemical shifts (δ) and coupling constants (J) are expressed in parts per million and hertz,

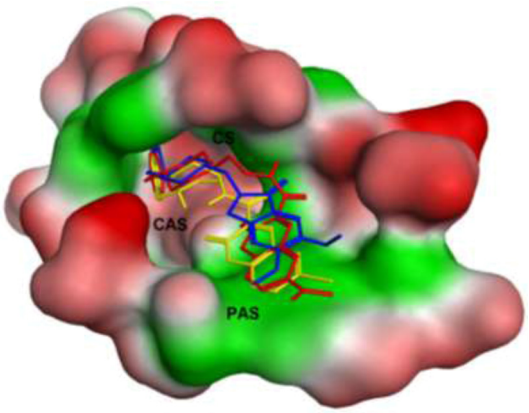

Fig. 3. Similar orientation of the best docked poses of **9b** (yellow) and **10c** (red) along with native ligand, donepezil (blue), in the active site of AChE. (For interpretation of the references to colour in this figure legend, the reader is referred to the web version of this article.)

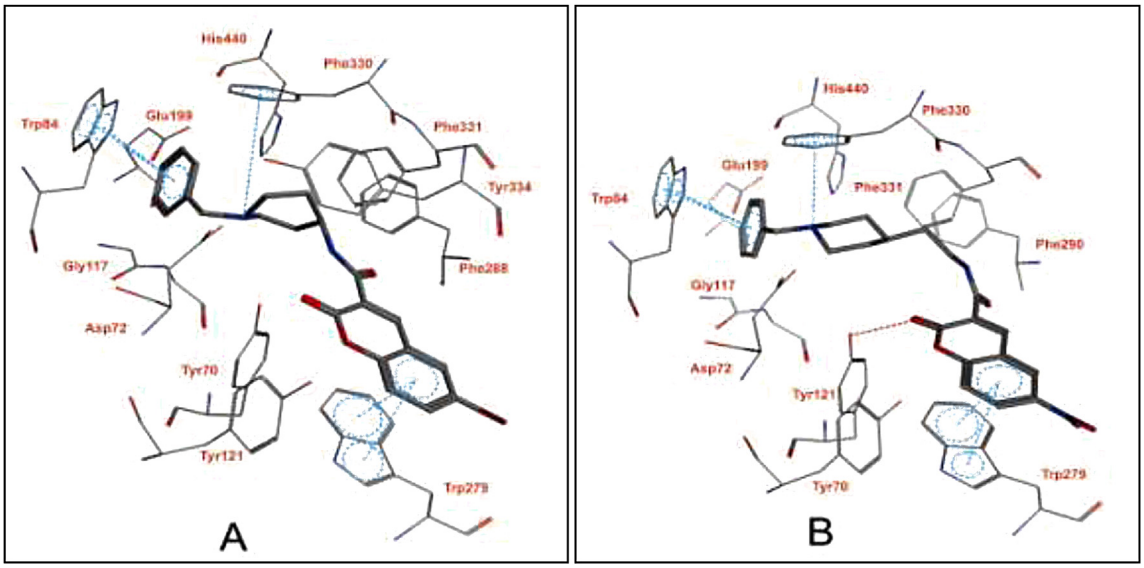

Fig. 4. Representative model for interactions of compounds **9b** (A) and **10c** (B) docked into the binding site of AChE. Hydrogen bond is indicated as red dotted line. (For interpretation of the references to colour in this figure legend, the reader is referred to the web version of this article.)

respectively. Mass spectroscopy was conducted with an HP (Agilent technologies) 5937 Mass Selective Detector. Elemental analyses were carried out by a CHN-Rapid Heraeus elemental analyzer. The results of elemental analyses (C, H, N) were within ±0.4% of the calculated values.

*4.1.1. General procedure for the preparation of compounds **9** and **10***

Compound **3** (1 mmol) was added to thionyl chloride (5 ml) and the mixture was refluxed for 3–5 h. After completion of the reaction, thionyl chloride was removed with simple distillation to give appropriate coumarin-3-carbonyl chloride derivative. The crude product was used directly without further purification. In the next step, appropriate amine (1-benzylpiperidin-4-amine or 2-(1-benzylpiperidin-4-yl)ethanamine) (1 mmol) and potassium carbonate (2 mmol) were dissolved in dry toluene (15 ml). The mixture was refluxed for 6–12 h, and then the solvent was removed under reduced pressure. The residue was purified by silica gel column chromatography using petroleum ether-ethyl acetate (8:2) as a mobile phase to give the pure product.

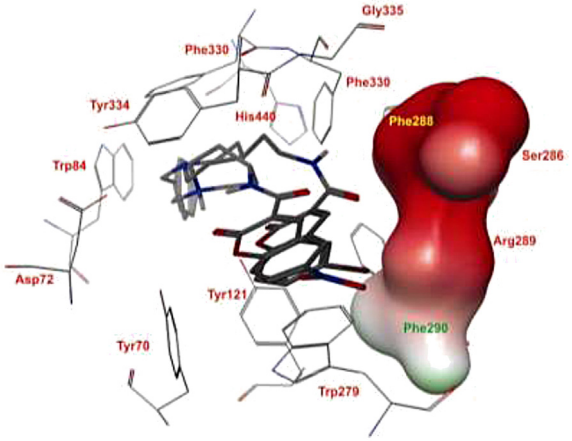

Fig. 5. The relative orientation of carboxamide linker of the best docking poses of **9b** and **10c**. The carboxamide linker of **10c** oriented to a hydrophillic pocket (red surface) of the active site. (For interpretation of the references to colour in this figure legend, the reader is referred to the web version of this article.)

*4.1.1.1. N-(1-Benzylpiperidin-4-yl)-2-oxo-2H-chromene-3-carboxamide (**9a**).* Yield: 65%; pale yellow solid; mp 198–200 °C; IR (KBr, cm^{-1}) ν_{max}: 3312 (NH), 1711 and 1648 (C=O). ^1H NMR (DMSO-d_6, 400 MHz) δ: 8.85 (s, 1H, H_4 coumarin), 8.63 (br s, 1H, NH), 7.99 (d, 1H, J = 7.5 Hz, H_5 coumarin), 7.75 (t, 1H, J = 7.5 Hz, H_7 coumarin), 7.51 (d, 1H, J = 7.5 Hz, H_8 coumarin), 7.44 (t, 1H, J = 7.5 Hz, H_6 coumarin), 7.32–7.22 (m, 5H Ph), 3.49 (s, 2H, CH_2 benzylic), 3.13–3.09 (m, 1H, NCH piperidine), 2.79–2.11 (m, 4H, $2CH_2N$ piperidine), 1.95–1.47 (m, 4H, $2\underline{CH_2}CH_2N$ piperidine). MS (*m*/*z*, %) 362 (M^+, 16), 271 (16), 189 (48), 173 (97), 91 (100). Anal. Calcd for $C_{22}H_{22}N_2O_3$: C, 72.91; H, 6.12; N, 7.73. Found: C, 72.74; H, 6.33; N, 7.51.

*4.1.1.2. N-(1-Benzylpiperidin-4-yl)-6-bromo-2-oxo-2H-chromene-3-carboxamide (**9b**).* Yield: 68%; pale yellow solid; mp 200–201 °C; IR (KBr, cm^{-1}) ν_{max}: 3319 (NH), 1716 and 1657 (C=O). ^1H NMR (DMSO-d_6, 400 MHz) δ: 8.78 (s, 1H, H_4 coumarin), 8.66 (br s, 1H, NH), 8.24 (d, 1H, J = 7.5 Hz, H_5 coumarin), 7.88 (d, 1H, J = 7.5 Hz, H_7 coumarin), 7.48 (d, 1H, J = 7.5 Hz, H_8 coumarin), 7.41–7.14 (m, 5H Ph), 3.85 (s, 2H, CH_2 benzylic), 3.63–3.60 (m, 1H, NCH piperidine), 2.87–2.13 (m, 4H, $2CH_2N$ piperidine), 1.98–1.59 (m, 2H, $2\underline{CH_2}CH_2N$ piperidine). MS (*m*/*z*, %) 442 (M + 2, 2), 440 (M^+, 2), 253 (22), 251 (21), 189 (55), 172 (77), 91 (100). Anal. Calcd for $C_{22}H_{21}BrN_2O_3$: C, 59.87; H, 4.80; N, 6.35. Found: C, 59.71; H, 4.65; N, 6.21.

*4.1.1.3. N-(1-Benzylpiperidin-4-yl)-6-nitro-2-oxo-2H-chromene-3-carboxamide (**9c**).* Yield: 66%; pale yellow solid; mp 224–225 °C; IR (KBr, cm^{-1}) ν_{max}: 3341 (NH), 1724 and 1656 (C=O), 1535, 1344 (NO_2). ^1H NMR (DMSO-d_6, 400 MHz) δ: 8.96 (s, 1H, H_5 coumarin), 8.62 (s, 1H, H_4 coumarin), 8.51 (d, 1H, J = 8.4 Hz, H_7 coumarin), 7.56 (d, 1H, J = 8.4 Hz, H_8 coumarin), 7.41–7.15 (m, 5H Ph), 4.05 (s, 2H, CH_2 benzylic), 3.64–3.54 (m, 1H, NCH piperidine), 2.88–2.04 (m, 4H, $2CH_2N$ piperidine), 1.79–1.25 (m, 4H, $2\underline{CH_2}CH_2N$ piperidine). MS (*m*/*z*, %) 407 (M^+, 3), 189 (31), 172 (51), 91 (100). Anal. Calcd for $C_{22}H_{21}N_3O_5$: C, 64.86; H, 5.20; N, 10.31. Found: C, 64.61; H, 5.08; N, 10.52.

*4.1.1.4. N-(1-Benzylpiperidin-4-yl)-7-methoxy-2-oxo-2H-chromene-3-carboxamide (**9d**).* Yield: 50%; pale yellow solid; mp 193–195 °C; IR (KBr, cm^{-1}) ν_{max}: 3311 (NH), 1705 and 1651 (C=O). ^1H NMR (DMSO-d_6, 400 MHz) δ: 8.80 (s, 1H, H_4 coumarin), 8.66 (br s, 1H, NH), 8.25 (d, 1H, J = 7.5 Hz, H_5 coumarin), 7.87 (d, 1H, J = 7.5 Hz, H_6

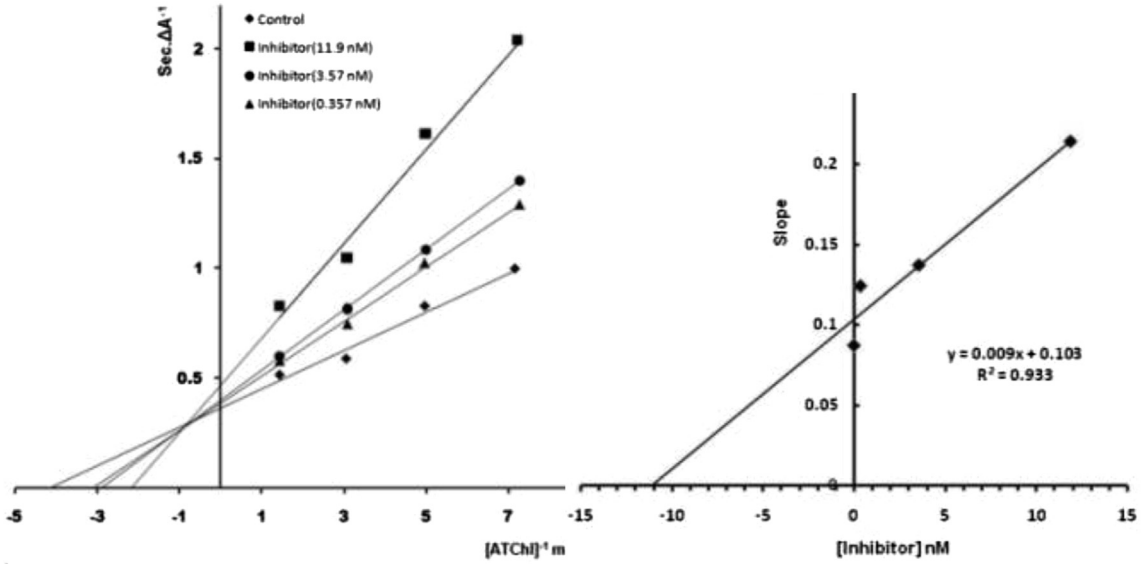

Fig. 6. Left: Lineweaver–Burk plot for the inhibition of AChE by **10c** at different concentrations with acetylthiocholine (ATCh) as substrate, Right: Steady-state inhibition constant (Ki) of **10c**.

coumarin), 7.35–7.54 (m, 5H Ph), 3.92 (s, 3H, OCH_3), 3.63 (s, 2H, CH_2 benzylic), 2.91–2.83 (m, 1H, NCH piperidine), 2.37–2.01 (m, 4H, $2CH_2N$ piperidine), 1.72–1.21 (m, 4H, $2\underline{CH_2}CH_2N$ piperidine). MS (*m*/*z*, %) 392 (M^+, 23), 365 (26), 290 (35), 178 (53), 129 (100). Anal. Calcd for $C_{23}H_{24}N_2O_4$: C, 70.39; H, 6.16; N, 7.14. Found: C, 70.51; H, 6.02; N, 7.21.

*4.1.1.5. N-(1-Benzylpiperidin-4-yl)-8-methoxy-2-oxo-2H-chromene-3-carboxamide (**9e**).* Yield: 76%; pale yellow solid; mp 198–200 °C; IR (KBr, cm^{-1}) ν_{max}: 3312 (NH), 1705 and 1648 (C=O). ^1H NMR (DMSO-d_6, 400 MHz) δ: 8.90 (s, 1H, H_4 coumarin), 8.84 (br s, 1H, NH), 7.72–7.64 (m, 2H, $H_{5,7}$ coumarin), 7.43–7.34 (m, 6H, 5H Ph and H_6 coumarin), 4.03 (s, 3H, OCH_3), 3.60–3.55 (m, 3H, CH_2 benzylic and NCH piperidine), 2.89–2.23 (m, 4H, $2CH_2N$ piperidine), 2.04–1.65 (m, 4H, $2\underline{CH_2}CH_2N$ piperidine). MS (*m*/*z*, %) 392 (M^+, 13), 260 (15), 203 (81), 172 (50), 91 (100), 77 (11). Anal. Calcd for $C_{23}H_{24}N_2O_4$: C, 70.39; H, 6.16; N, 7.14. Found: C, 70.51; H, 6.22; N, 7.31.

*4.1.1.6. N-(1-Benzylpiperidin-4-yl)-7-hydroxy-2-oxo-2H-chromene-3-carboxamide (**9f**).* Yield: 55%; pale yellow solid; mp 185–186 °C; IR (KBr, cm^{-1}) ν_{max}: 3439 (OH), 3232 (NH), 1714 and 1646 (C=O). ^1H NMR (DMSO-d_6, 400 MHz) δ: 8.77 (s, 1H, H_4 coumarin), 8.59 (br s, 1H, NH), 7.81 (d, 1H, J = 7.5 Hz, H_5 coumarin), 7.39–7.11 (m, 5H Ph), 6.87–6.80 (m, 2H, $H_{6,8}$ coumarin), 3.83 (s, 2H, CH_2 benzylic), 3.53–3.51 (m, 1H, NCH piperidine), 2.78–2.11 (m, 4H, $2CH_2N$ piperidine), 1.89–1.50 (m, 4H, $2\underline{CH_2}CH_2N$ piperidine). MS (*m*/*z*, %) 378 (M^+, 11), 287 (42), 189 (51), 172 (70), 91 (100). Anal. Calcd for $C_{22}H_{22}N_2O_4$: C, 69.83; H, 5.86; N, 7.40. Found: C, 69.67; H, 5.98; N, 7.27.

*4.1.1.7. N-[2-(1-Benzylpiperidin-4-yl)ethyl]-2-oxo-2H-chromene-3-carboxamide (**10a**).* Yield: 53%; pale yellow solid; mp 145–146 °C; IR (KBr, cm^{-1}) ν_{max}: 3350 (NH), 1712 and 1650 (C=O). ^1H NMR (DMSO-d_6, 500 MHz) δ: 8.84 (s, 1H, H_4 coumarin), 8.66 (br s, 1H, NH), 7.98 (d, 1H, J = 7.5 Hz, H_5 coumarin), 7.75 (t, 1H, J = 7.5 Hz, H_7 coumarin), 7.50 (d, 1H, J = 7.5 Hz, H_8 coumarin), 7.44 (t, 1H, J = 7.5 Hz, H_6 coumarin), 7.32–7.22 (m, 5H Ph), 3.45–3.38 (m, 4H, NCH_2 and CH_2 benzylic), 2.82–2.71 (m, 2H, 2CHN piperidine), 1.84–1.98 (m, 2H, 2CHN piperidine), 1.74–1.63 (m, 2H, $2\underline{CH}CH_2N$ piperidine), 1.49–1.46 (m, 2H, $NHCH_2\underline{CH_2}$), 1.23–1.11 (m, 3H, $\underline{CH}CH_2CH_2N$ piperidine and $2\underline{CH}CH_2N$ piperidine). MS (*m*/*z*, %) 390 (M^+, 15), 299 (50), 217 (98), 173 (44), 91 (100). Anal. Calcd for $C_{24}H_{26}N_2O_3$: C, 73.82; H, 6.71; N, 7.17. Found: C, 73.64; H, 6.51; N, 7.21.

*4.1.1.8. N-[2-(1-Benzylpiperidin-4-yl)ethyl]-6-bromo-2-oxo-2H-chromene-3-carboxamide (**10b**).* Yield: 55%; pale yellow solid; mp 189–190 °C; IR (KBr, cm^{-1}) ν_{max}: 3342 (NH), 1712 and 1651 (C=O). ^1H NMR (DMSO-d_6, 400 MHz) δ: 8.80 (s, 1H, H_4 coumarin), 8.66 (s, 1H, H_5 coumarin), 8.26 (br s, 1H, NH), 7.88 (d, J = 7.5 Hz, 1H, H_7 coumarin), 7.58–7.25 (m, 6H, 5H Ph and H_8 coumarin), 3.56 (s, 2H, CH_2 benzylic), 3.09–3.01 (m, 2H, $NHCH_2$), 2.79–2.62 (m, 2H, 2CHN piperidine), 2.25–2.11 (m, 2H, 2CHN piperidine), 2.09–2.00 (m, 2H, $2\underline{CH}CH_2N$ piperidine), 1.81–1.62 (m, 2H, $NCH_2\underline{CH_2}$), 1.59–1.32 (m, 3H, $\underline{CH}CH_2CH_2N$ piperidine and $2\underline{CH}CH_2N$ piperidine). MS (*m*/*z*, %) 470 (M + 2, 12), 468 (M^+, 13), 379 (15), 377 (13), 217 (98), 172 (15), 91 (100). Anal. Calcd for $C_{24}H_{25}BrN_2O_3$: C, 61.41; H, 5.37; N, 5.97. Found: C, 61.31; H, 5.52; N, 5.72.

*4.1.1.9. N-[2-(1-Benzylpiperidin-4-yl)ethyl]-6-nitro-2-oxo-2H-chromene-3-carboxamide (**10c**).* Yield: 75%; pale yellow solid; mp 199–200 °C; IR (KBr, cm^{-1}) ν_{max}: 3340 (NH), 1724 and 1651 (C=O), 1531 and 1344 (NO_2). ^1H NMR (DMSO-d_6, 400 MHz) δ: 8.97 (br s, 2H, $H_{4,5}$ coumarin), 8.63 (br s, 1H, NH), 8.51 (d, 1H, J = 7.5 Hz, H_7 coumarin), 7.72 (d, 1H, J = 7.5 Hz, H_8 coumarin), 7.58–7.31 (m, 5H Ph), 3.63 (s, 2H, CH_2 benzylic), 3.11–3.02 (m, 2H, $N\underline{CH_2}$), 2.81–2.64 (m, 2H, 2CHN piperidine), 2.27–2.13 (m, 2H, 2CHN piperidine), 2.09–2.00 (m, 2H, $2\underline{CH}CH_2N$ piperidine), 1.80–1.61 (m, 2H, $NCH_2\underline{CH_2}$), 1.58–1.31 (m, 3H, $\underline{CH}CH_2CH_2N$ piperidine and $2\underline{CH}CH_2N$ piperidine). MS (*m*/*z*, %) 435 (M^+, 10), 344 (16), 217 (100), 172 (22), 91 (83). Anal. Calcd for $C_{24}H_{25}N_3O_5$: C, 66.19; H, 5.79; N, 9.65. Found: C, 66.33; H, 5.51; N, 9.44.

*4.1.1.10. N-[2-(1-Benzylpiperidin-4-yl)ethyl]-6-hydroxy-2-oxo-2H-chromene-3-carboxamide (**10d**).* Yield: 53%; pale yellow solid; mp 185–186 °C; IR (KBr, cm^{-1}) ν_{max}: 3413 (OH), 3313 (NH), 1701 and 1642 (C=O). ^1H NMR (DMSO-d_6, 500 MHz) δ: 8.96 (br s, 1H, NH), 8.76 (s, 1H, H_4 coumarin), 7.31–7.23 (m, 6H, 5H Ph and H_8 coumarin), 7.14 (d, 1H, J = 7.5 Hz, H_7 coumarin), 7.05 (s, 1H, H_5

coumarin), 3.52 (s, 2H, CH_2 benzylic), 3.45–3.38 (m, 2H, NCH_2), 2.96–2.92 (m, 2H, 2CHN piperidine), 2.02–2.00 (m, 2H, 2CHN piperidine), 1.74–1.69 (m, 3H, $CHCH_2CH_2N$ piperidine and $2CHCH_2N$ piperidine), 1.60–1.55 (m, 4H, NCH_2CH_2 and $2CHCH_2N$ piperidine). MS (*m*/*z*, %) 406 (M^+, 7), 315 (33), 217 (53), 189 (38), 106 (36), 91 (100). Anal. Calcd for $C_{24}H_{26}N_2O_4$: C, 70.92; H, 6.45; N, 6.89. Found: C, 70.78; H, 6.33; N, 6.71.

*4.1.1.11. N-[2-(1-Benzylpiperidin-4-yl)ethyl]-7-methoxy-2-oxo-2H-chromene-3-carboxamide (**10e**).* Yield: 65%; pale yellow solid; mp 168–169 °C; IR (KBr, cm^{-1}) ν_{max}: 3360 (NH), 1706 and 1646 (C=O). ^1H NMR (DMSO-d_6, 400 MHz) δ: 8.80 (s, 1H, H_4 coumarin), 8.75 (br s, 1H, NH), 7.59–7.57 (m, 3H, 2H Ph, H_5 coumarin), 7.25–7.23 (m, 3H Ph), 6.94 (d, 1H, J = 7.5 Hz, H_6 coumarin), 6.86 (s, 1H, H_8 coumarin), 4.08 (s, 2H, CH_2 benzylic), 3.91 (s, 3H, OCH_3), 3.57–3.28 (m, 4H, NCH_2 and 2CHN piperidine), 2.60–2.52 (m, 2H, 2CHN piperidine), 2.05–1.92 (m, 2H, $2CHCH_2N$ piperidine), 1.79–1.45 (m, 3H, NCH_2CH_2 and $CHCH_2CH_2N$ piperidine), 1.27–1.22 (m, 2H, $2CHCH_2N$ piperidine). MS (*m*/*z*, %) 420 (M^+, 9), 404 (5), 388 (23), 172 (26), 91 (100). Anal. Calcd for $C_{25}H_{28}N_2O_4$: C, 71.41; H, 6.71; N, 6.66. Found: C, 71.33; H, 6.87; N, 6.45.

*4.1.1.12. N-[2-(1-Benzylpiperidin-4-yl)ethyl]-7-hydroxy-2-oxo-2H-chromene-3-carboxamide (**10f**).* Yield: 62%; pale yellow solid; mp 185–186 °C; IR (KBr, cm^{-1}) ν_{max}: 3449 (OH), 3328 (NH), 1720 and 1648 (C=O). ^1H NMR (DMSO-d_6, 500 MHz) δ: 8.89 (br s, 1H, NH), 8.77 (s, 1H, H_4 coumarin), 7.58 (d, 1H, J = 7.5 Hz, H_5 coumarin), 7.29–7.24 (m, 5H, Ph), 6.86–6.81 (m, 2H, H_6 and H_8 coumarin), 3.61 (s, 2H, CH_2 benzylic), 3.50–3.41 (m, 2H, NCH_2), 2.66–2.61 (m, 2H, 2CHN piperidine), 2.04–2.00 (m, 2H, 2CHN piperidine), 1.92–1.87 (m, 3H, $CHCH_2CH_2N$ piperidine and $2CHCH_2N$ piperidine), 1.60–1.54 (m, 4H, NCH_2CH_2 and $2CHCH_2N$ piperidine). MS (*m*/*z*, %) 406 (M^+, 14), 315 (40), 217 (83), 189 (33), 172 (21), 91 (100). Anal. Calcd for $C_{24}H_{26}N_2O_4$: C, 70.92; H, 6.45; N, 6.89. Found: C, 70.98; H, 6.63; N, 7.11.

*4.1.1.13. N-[2-(1-Benzylpiperidin-4-yl)ethyl]-8-methoxy-2-oxo-2H-chromene-3-carboxamide (**10g**).* Yield: 72%; pale yellow solid; mp 212–213 °C; IR (KBr, cm^{-1}) ν_{max}: 3340 (NH), 1736 and 1660 (C=O). ^1H NMR (DMSO-d_6, 400 MHz) δ: 8.97 (s, 1H, H_4 coumarin), 8.63–8.57 (m, 2H, NH and H_6 coumarin), 8.51 (d, 1H, J = 8.4 Hz, H_5 coumarin), 7.55 (d, 1H, J = 8.4 Hz, H_7 coumarin), 7.39–7.31 (m, 5H Ph), 3.61 (s, 2H, CH_2 benzylic), 3.51 (s, 3H, OCH_3), 3.09–2.95 (m, 2H, $NHCH_2$), 2.18–2.04 (m, 2H, 2CHN piperidine), 1.78–1.72 (m, 2H, 2CHN piperidine), 1.64–1.59 (m, 2H, $2CHCH_2N$ piperidine), 1.47–1.40 (m, 2H, NCH_2CH_2), 1.27–1.22 (m, 3H, $CHCH_2CH_2N$ piperidine and $2CHCH_2N$ piperidine). MS (*m*/*z*, %) 420 (M^+, 5), 217 (91), 172 (39), 106 (36), 91 (100). Anal. Calcd for $C_{25}H_{28}N_2O_4$: C, 71.41; H, 6.71; N, 6.66. Found: C, 71.27; H, 6.61; N, 6.45.

4.2. Molecular modeling studies

The conformational search studies were performed with HyperChem7 (Hypercube Inc.) using AM1 semi-empirical method. For the docking procedure, the pdb structure of 1EVE was taken from the Brookhaven protein database (http://www.rcsb.org) as a complex bound with inhibitor E2020 (donepezil). Afterward, the water molecules and co-crystallized ligand were eliminated from the protein structure and polar hydrogens were added. The Kollman charge was calculated and the protein was saved as pdbqt format. The structure of the target compounds was prepared using MarvineSketch 5.8.3, 2012, ChemAxon (http://www.chemaxon.com) and converted to 3D pdbqt coordinates by Openbabel version (2.3.1) [19]. The autodock format of protein was also prepared using Autodock Tools (ver. 1.5.4) [20]. Docking simulations were finally carried out by means of a batch script using Autodock vina (ver. 1.1.1) [21] with default parameters and the exhaustiveness value set as 80. The active site for docking was established as a box at geometrical center of the native ligand present in the above mentioned PDB structure with the dimensions 40,40,40. The coordinates *x*, *y*, *z*, for the center of grid box were set as 2.023, 63.29 and 67.062, respectively. The lowest energy conformation of each ligand–enzyme complex was selected for analyzing the interactions between AChE and the inhibitor. The results were visualized using Chimera 1.6 [22] (Molecular graphics and analyses were performed with the UCSF Chimera package. Chimera is developed by the Resource for Biocomputing, Visualization, and Informatics at the University of California, San Francisco).

4.3. AChE and BuChE inhibition assay

Acetylcholinesterase (AChE, E.C. 3.1.1.7, Type V-S, lyophilized powder, from *electric eel*, 1000 unit), butyrylcholinesterase (BuChE, E.C. 3.1.1.8, from equine serum) and butyrylthiocholine iodide (BTC) were provided from Sigma–Aldrich. 5,5-Dithiobis-(2-nitrobenzoic acid) (DTNB), potassium dihydrogen phosphate, dipotassium hydrogen phosphate, potassium hydroxide, sodium hydrogen carbonate, and acetylthiocholine iodide were purchased from Fluka. The solutions of the target compounds were prepared in a mixture of DMSO (1 ml) and methanol (9 ml) and diluted in 0.1 M KH_2PO_4/K_2HPO_4 buffer (pH 8.0) to obtain final assay concentrations. The temperature condition was adjusted as 25 °C during all experiments. Five different concentrations were tested for each compound in triplicate to obtain the range of 20%–80% inhibition for AChE and BuChE. The assay medium was composed of 3 ml of 0.1 M phosphate buffer pH 8.0, 100 μl of 0.01 M DTNB, and 100 μl of 2.5 unit/mL enzyme solution (AChE, E.C. 3.1.1.7, Type V-S, lyophilized powder, from *electric eel*). 100 μl of each tested compound was added to the assay tube and incubated at 25 °C for 15 min prior to adding 20 μl of substrate (acetylthiocholine iodide). The rate of absorbance change was measured at 412 nm for 6 min on the baseline obtained by blank reading of the solutions with non-enzymatic hydrolysis. The blank was contained 3 ml buffer, 200 μl water, 100 μl DTNB and 20 μl substrate. The IC_{50} values were determined graphically from inhibition curves (log inhibitor concentration versus percent of inhibition). Spectrophotometric measurements were performed on a UV Unico Double Beam Spectrophotometer [23]. The described method was also taken for BuChE inhibition assay.

4.4. Cellular biology

4.4.1. Cell culture, differentiation, and treatment conditions

Rat undifferentiated PC12 cells were cultured in RPMI 1640 media with 10% FCS containing 100 units/ml penicillin and 100 μg/ml streptomycin (All from GIBCO, Grand Island, NY, USA). Cells were trypsinated and 10^4 cells were plated on each well of 96-well culture plates in RPMI 1640 media. For induction of neuronal differentiation, PC12 cells were cultured in serum-free media (RPMI 1640 media containing 100 units/ml penicillin and 100 μg/ml streptomycin) for 2 days, thereafter their medium changed to above serum free medium containing NGF (50 ng/ml, Sigma) and continued for 5 days until neurite outgrowth was observed under inverted microscope (Supplementary material) [24]. Differentiated PC12 cells were pretreated with different concentrations (1, 10 and 100 μM) of the compounds for 3 h before treatment with H_2O_2 (250 μM). The occurrence of apoptosis was established after staining with DAPI, and cell viability was measured after 24 h by using the MTT assay.

4.4.2. Measurement of cell viability with MTT assay

Cells were plated at a density of 10^4 cells/well in the 96-well plate, cultured, differentiated and treated as described above. 10 μl of MTT (Sigma) with the concentration of 5 mg/ml was added to the cell culture media (150 μl) and incubated in CO_2 incubator for 3.5 h. Thereafter, medium and MTT solution was removed and DMSO (150 μl) was added into the each well and the formazan precipitates were dissolved by shaking the plate for 10 min on shaker with the speed of 120 rpm. Finally optical density (OD) was evaluated at 560 nm on the ELISA plate reader. Results were compensated with OD measured in the same conditioned well without adding MTT [25].

4.4.3. DAPI staining to evaluate apoptosis induction

DAPI staining was accomplished to evaluate the effect of H_2O_2 on induction of apoptosis. For this purpose the differentiated PC12 cells were cultured in 96 well plate and treated with different doses of drugs as indicated above and stained with the DNA-specific fluorochrome 4′,6-diamidino-2-phenylindole dihydrochloride (DAPI, Sigma). DAPI was added to the culture medium of live cells with the final concentration of 1 μg/ml for 20 min. Because the cell membrane of apoptotic cell is permeable, DAPI enters into the cell and stains the nucleus, while normal cell is not permeable sufficiently and gets lightly stained (Supplementary material) [24].

Acknowledgments

This research was supported by grants from the Research Council of Tehran University of Medical Sciences and the Iran National Science Foundation (INSF).

Appendix A. Supplementary data

Supplementary data related to this article can be found at http://dx.doi.org/10.1016/j.ejmech.2013.10.024.

References

[1] H.W. Querfurth, F.M. LaFerla, Alzheimer's disease, N. Engl. J. Med. 362 (2010) 329–344.
[2] A.V. Terry Jr., J.J. Buccafusco, The cholinergic hypothesis of age and Alzheimer's disease-related cognitive deficits: recent challenges and their implications for novel drug development, J. Pharmacol. Exp. Ther. 306 (2003) 821–827.
[3] D.J. Selkoe, Alzheimer's disease: genes, proteins, and therapy, Physiol. Rev. 81 (2001) 741–766.
[4] E. Giacobini, Cholinesterase inhibitors: new roles and therapeutic alternatives, Pharmacol. Res. 50 (2004) 433–440.
[5] M. Decker, B. Kraus, J. Heilmann, Design, synthesis and pharmacological evaluation of hybrid molecules out of quinazolinimines and lipoic acid lead to highly potent and selective butyrylcholinesterase inhibitors with antioxidant properties, Bioorg. Med. Chem. 16 (2008) 4252–4261.
[6] M.A. Kamal, P. Klein, W. Luo, Y. Li, H.W. Holloway, D. Tweedie, N.H. Greig, Kinetics of human serum butyrylcholinesterase inhibition by a novel experimental Alzheimer therapeutic, dihydrobenzodioxepine cymserine, Neurochem. Res. 33 (2008) 745–753.
[7] H. Sugimoto, Y. Yamanishi, Y. Iimura, Y. Kawakami, Donepezil hydrochloride (E2020) and other acetylcholinesterase inhibitors, Curr. Med. Chem. 7 (2000) 303–339.
[8] S. Kavanagh, M. Gaudig, B.B. Van, M. Adami, A. Delgado, C. Guzman, E. Jedenius, B. Schäuble, Galantamine and behavior in Alzheimer disease: analysis of four trials, Acta Neurol. Scand. 124 (2011) 302–308.
[9] R. Hoerr, M. Noeldner, Ensaculin (KA-672 HCl): a multitransmitter approach to dementia treatment, CNS Drug Rev. 8 (2002) 143–158.
[10] P. Anand, B. Singh, N. Singh, A review on coumarins as acetylcholinesterase inhibitors for Alzheimer's disease, Bioorg. Med. Chem. 20 (2012) 1175–1180.
[11] C. Dan, P. Ya-fei, L. Chuan-jun, X. Yun-feng, J. Yu-ren, Virtual screening of acetylcholinesterase inhibitors, in: M. Taha (Ed.), Virtual Screening, InTech Publisher, Shanghi, 2012, pp. 83–90.
[12] N. Duval, S. Bon, I. Silman, J. Sussman, J. Massoulie, Site-directed mutagenesis of active-site-related residues in Torpedo acetylcholinesterase. Presence of a glutamic acid in the catalytic triad, FEBS Lett. 309 (1992) 421–423.
[13] F. Leonetti, M. Catto, O. Nicolotti, L. Pisani, A. Cappa, A. Stefanachi, A. Carotti, Homo- and hetero-bivalent edrophonium-like ammonium salts as highly potent, dual binding site AChE inhibitors, Bioorg. Med. Chem. 16 (2008) 7450–7456.
[14] M. Catto, L. Pisani, F. Leonetti, O. Nicolotti, P. Pesce, A. Stefanachi, S. Cellamare, A. Carotti, Design, synthesis and biological evaluation of coumarin alkylamines as potent and selective dual binding site inhibitors of acetylcholinesterase, Bioorg. Med. Chem. 21 (2013) 146–152.
[15] M. Alipour, M. Khoobi, A. Foroumadi, H. Nadri, A. Moradi, A. Sakhteman, M. Ghandi, A. Shafiee, Novel coumarin derivatives bearing *N*-benzyl pyridinium moiety: potent and dual binding site acetylcholinesterase inhibitors, Bioorg. Med. Chem. 20 (2012) 7214–7222.
[16] X. Zhou, X.B. Wang, T. Wang, L.Y. Kong, Design, synthesis, and acetylcholinesterase inhibitory activity of novel coumarin analogues, Bioorg. Med. Chem. 16 (2008) 8011–8021.
[17] D. Shao, C. Zou, C. Luo, X. Tang, Y. Li, Synthesis and evaluation of tacrine-E2020 hybrids as acetylcholinesterase inhibitors for the treatment of Alzheimer's disease, Bioorg. Med. Chem. Lett. 14 (2004) 4639–4642.
[18] A. Rampa, A. Bisi, F. Belluti, S. Gobbi, P. Valenti, V. Andrisano, V. Cavrini, A. Cavalli, M. Recanatini, Acetylcholinesterase inhibitors for potential use in Alzheimer's disease: molecular modeling, synthesis and kinetic evaluation of 11*H*-indeno-[1,2-*b*]-quinolin-10-ylamine derivatives, Bioorg. Med. Chem. 8 (2000) 497–506.
[19] N.M. O'Boyle, M. Banck, C.A. James, C. Morley, T. Vandermeersch, G.R. Hutchison, Open Babel: an open chemical toolbox, J. Cheminf. 3 (2011) 33.
[20] M.F. Sanner, Python: a programming language for software integration and development, J. Mol. Graph. Model. 17 (1999) 57–61.
[21] O. Trott, A.J. Olson, AutoDock Vina: improving the speed and accuracy of docking with a new scoring function, efficient optimization, and multithreading, J. Comput. Chem. 31 (2010) 455–461.
[22] E.F. Pettersen, T.D. Goddard, C.C. Huang, G.S. Couch, D.M. Greenblatt, E.C. Meng, T.E. Ferrin, UCSF Chimera – a visualization system for exploratory research and analysis, J. Comput. Chem. 25 (2004) 1605–1612.
[23] H. Nadri, M. Pirali-Hamedani, A. Moradi, A. Sakhteman, A. Vahidi, V. Sheibani, A. Asadipour, N. Hosseinzadeh, M. Abdollahi, A. Shafiee, A. Foroumadi, 5,6-Dimethoxybenzofuran-3-one derivatives: a novel series of dual acetylcholinesterase/butyrylcholinesterase inhibitors bearing benzyl pyridinium moiety, Daru J. Pharm. Sci. 21 (2013) 15.
[24] S.H. Koh, S.H. Kim, H. Kwon, Y. Park, K.S. Kim, C.W. Song, J. Kim, M.H. Kim, H.J. Yu, J.S. Henkel, H.K. Jung, Epigallocatechin gallate protects nerve growth factor differentiated PC12 cells from oxidative-radical-stress-induced apoptosis through its effect on phosphoinositide 3-kinase/Akt and glycogen synthase kinase-3, Brain Res. Mol. Brain Res. 118 (2003) 72–81.
[25] D. Zsolt, A. Juhász, M. Gálfi, K. Soós, R. Papp, D. Zádori, B. Penke, Method for measuring neurotoxicity of aggregating polypeptides with the MTT assay on differentiated neuroblastoma cells, Brain Res. Bull. 62 (2003) 223–229.